The human macrophage mannose receptor directs *Mycobacterium tuberculosis* lipoarabinomannan-mediated phagosome biogenesis

Peter B. Kang,[2] Abul K. Azad,[1] Jordi B. Torrelles,[1] Thomas M. Kaufman,[2] Alison Beharka,[2] Eric Tibesar,[2] Lucy E. DesJardin,[2] and Larry S. Schlesinger[1]

[1]Division of Infectious Diseases, Departments of Internal Medicine and Molecular Virology, Immunology, and Medical Genetics, and the Center for Microbial Interface Biology, The Ohio State University, Columbus, OH 43210
[2]Division of Infectious Diseases, Departments of Internal Medicine and Microbiology, the Immunology Program, and the VA Medical Center, The University of Iowa, Iowa City, IA 52242

***Mycobacterium tuberculosis* (*M.tb*) survives in macrophages in part by limiting phagosome–lysosome (P-L) fusion. *M.tb* mannose-capped lipoarabinomannan (ManLAM) blocks phagosome maturation. The pattern recognition mannose receptor (MR) binds to the ManLAM mannose caps and mediates phagocytosis of bacilli by human macrophages. Using quantitative electron and confocal microscopy, we report that engagement of the MR by ManLAM during the phagocytic process is a key step in limiting P-L fusion. P-L fusion of ManLAM microspheres was significantly reduced in human macrophages and an MR-expressing cell line but not in monocytes that lack the receptor. Moreover, reversal of P-L fusion inhibition occurred with MR blockade. Inhibition of P-L fusion did not occur with entry via Fcγ receptors or dendritic cell–specific intracellular adhesion molecule 3 grabbing nonintegrin, or with phosphatidylinositol-capped lipoarabinomannan. The ManLAM mannose cap structures were necessary in limiting P-L fusion, and the intact molecule was required to maintain this phenotype. Finally, MR blockade during phagocytosis of virulent *M.tb* led to a reversal of P-L fusion inhibition in human macrophages (84.0 ± 5.1% vs. 38.6 ± 0.6%). Thus, engagement of the MR by ManLAM during the phagocytic process directs *M.tb* to its initial phagosomal niche, thereby enhancing survival in human macrophages.**

CORRESPONDENCE
Larry S. Schlesinger:
schlesinger-2@medctr.osu.edu

Abbreviations used: DC-SIGN, DC-specific intracellular adhesion molecule 3 grabbing nonintegrin; dManLAM, deacylated ManLAM; HSA, human serum albumin; LM, lipomannan; ManLAM, mannose-capped lipoarabinomannan; MDM, monocyte-derived macrophages; MOI, multiplicity of infection; MR, mannose receptor; *M.tb*, *Mycobacterium tuberculosis*; PILAM, phosphatidyl-*myo*-inositol capped lipoarabinomannan; P-L, phagosome–lysosome; PRR, pattern recognition receptor; TEM, transmission electron microscopy.

Mycobacterium tuberculosis (*M.tb*) has developed multiple strategies to enhance its entry and intracellular survival in mononuclear phagocytes by engaging a defined set of phagocytic receptors, thereby initiating specific signaling pathways and modulating several immunobiological processes during and after phagocytosis (1). A prominent mannose-containing lipoglycan of the *M.tb* cell wall, the terminal mannose-capped lipoarabinomannan (ManLAM) (2), has been directly implicated in the regulation of several of these processes (3). The presence of ManLAM on the mycobacterial surface (4) places this molecule in an ideal position to mediate the initial interactions between *M.tb* and macrophages.

P.B. Kang and A.K. Azad contributed equally to this work.
P.B. Kang's present address is Division of Science and Research Institute, American Dental Association, Chicago, IL 60611.
L.E. DesJardin's present address is University Hygienic Laboratory, University of Iowa, Iowa City, IA 52242.

After phagocytosis, *M.tb* resides in a phagosome that does not mature into a phagolysosome, considered a critical aspect of disease pathogenesis (5, 6). The biochemical mechanisms underlying this phenomenon have begun to be elucidated (7, 8). ManLAM has been shown to be a critical regulator of phagosome maturation in murine macrophages and a human monocytic cell line (8, 9). ManLAM blocks the increase of macrophage cytosolic Ca^{2+} and thereby inhibits interaction of the phosphatidylinositol 3 kinase (PI3K), hVPS34, with calmodulin, a step necessary for the production of PI3-phosphate involved in the recruitment of the Rab5 effector early endosomal antigen 1 to phagosomes. Early endosomal antigen 1 is necessary for the delivery of lysosomal components from the trans-Golgi network to the phagosome and regulates fusion of phagosomes with vesicles of the endosomal–lysosomal pathway (10).

The Journal of Experimental Medicine

For professional phagocytes such as macrophages, the time frame from the phagocytosis of a microbe to the maturation of its phagosome is short (11). Thus it is critical to explore the phagocytic process itself in initiating the development of the unique phagosome of *M.tb*. Macrophages have evolved a restricted number of phagocytic receptors, termed pattern recognition receptors (PRRs), which recognize conserved motifs, commonly carbohydrates, on the surface of microbes (12). Such receptors include the C-type lectins mannose receptor (MR) and DC-specific intracellular adhesion molecule 3 grabbing nonintegrin (DC-SIGN), among others (13). Human macrophages primarily use the MR as well as complement receptor 3 for the phagocytosis of *M.tb* (14). These receptors are distinguished by the fact that they mediate the engulfment of microbes without necessarily inciting a proinflammatory response (11) and thereby have long been postulated to enhance early intracellular survival of the microbe.

We have previously determined that the terminal mannose caps of *M.tb* ManLAM engage the MR during the phagocytic process by human macrophages (15). ManLAM caps also bind to DC-SIGN on DCs (16, 17). In contrast, phosphatidyl-*myo*-inositol capped lipoarabinomannan (PILAM) from avirulent *Mycobacterium smegmatis* does not engage the MR (15) or DC-SIGN (16), but rather TLR2, thereby activating a proinflammatory response (18). Thus, the terminal components of ManLAM are very important in host cell recognition and response. The fact that the MR-dependent phagocytosis is associated with an anti-inflammatory program and is not coupled with activation of the NADPH oxidase (19, 20), together with evidence that ManLAM inhibits IL-12 production via the MR by generating a negative signal in the cell (21), provides support for the preferential use of the MR-ManLAM pathway in macrophages by *M.tb*.

Because the involvement of specific receptors has been linked to phagosomal trafficking (22–25), we explored whether following engagement of ManLAM the MR initiates a phagocytic process that results in a phagosome with altered fusogenic properties. We report the first evidence that MR-mediated phagocytosis by primary human macrophages directs ManLAM and *M.tb* bacilli to a phagosomal compartment that has limited fusion with lysosomes. We show that the influence of the MR is specific and sufficient in its effect and that its engagement by the terminal mannose caps of ManLAM plays an important role in this process. These studies indicate that by regulating the earliest phagosomal traffic following phagocytosis, the MR phagocytic pathway enables ManLAM-containing *M.tb* to escape P-L fusion to establish its residence in the cell.

RESULTS

ManLAM-mediated phagocytosis by human macrophages results in limited P-L fusion

To assess the role of ManLAM in regulating P-L fusion in primary human macrophages, ManLAM (from the virulent

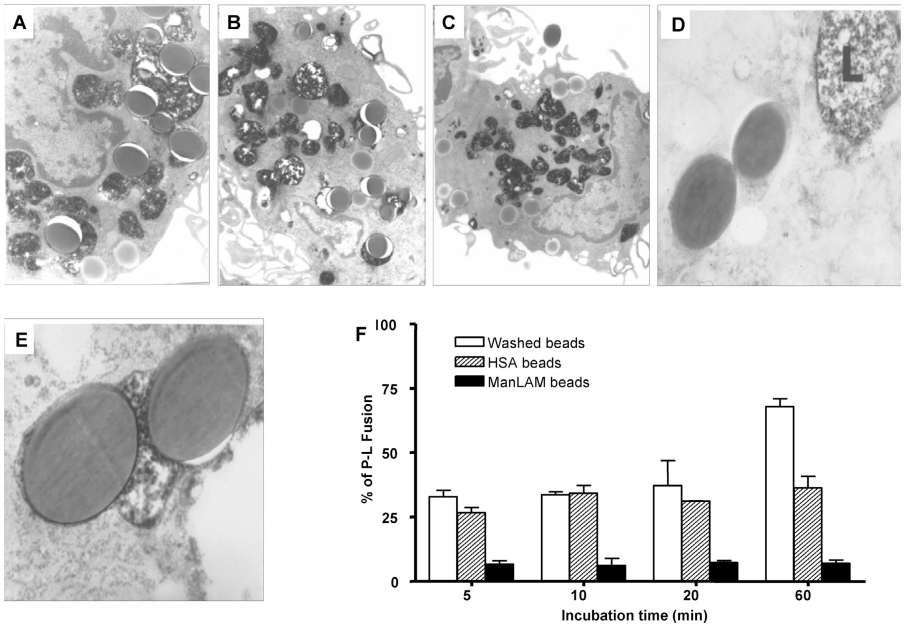

Figure 1. ManLAM bead phagosomes demonstrate limited fusion with lysosomes in macrophages after phagocytosis. Low-power electron micrographs of P-L fusion events using (A) washed beads (×24,000), (B) HSA beads (×14,000) and (C) ManLAM beads (×12,000). Lysosomes contain black particulate material. High-power electron micrographs of (D) ManLAM bead phagosomes shown with a neighboring lysosome (L) that is not fused (×40,000), and of (E) washed beads fused with lysosomes forming a phagolysosome (×60,000). (F) Extent of P-L fusion of washed, HSA, and ManLAM bead phagosomes. MDMs in monolayer culture were pulsed/chased with 1 mg/ml horseradish peroxidase for 2 h at 37°C. A synchronized phagocytosis assay was performed for the indicated times. After fixation, MDMs were processed for TEM. The percentage of P-L fusion (mean ± SEM, $n = 2$) was significantly reduced with ManLAM beads compared with both washed and HSA bead controls ($P < 0.005$; one-way ANOVA).

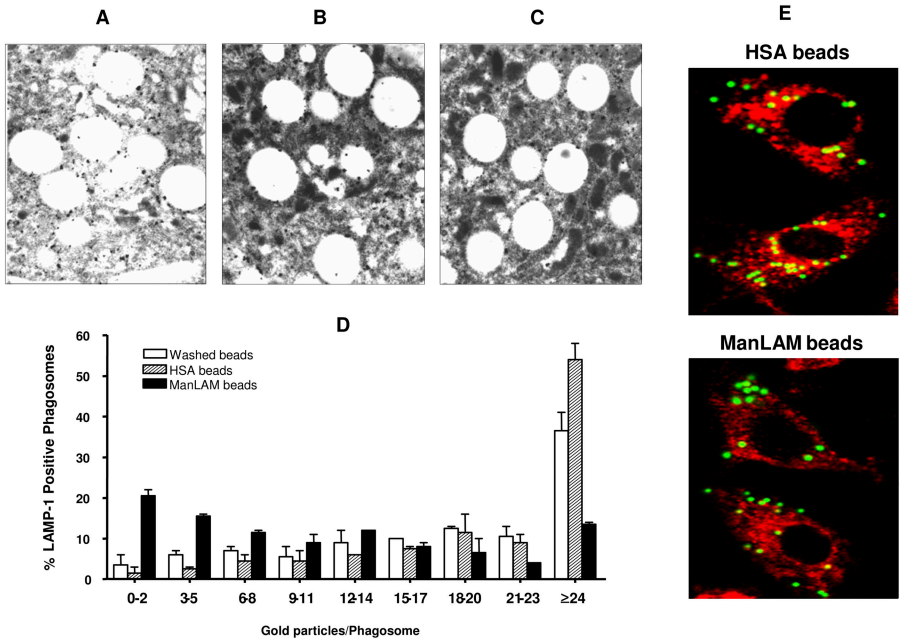

Figure 2. LAMP-1 staining on ManLAM bead phagosomes in macrophages is reduced. Electron micrographs (×20,000) of (A) washed and (B) HSA bead phagosomes show higher levels of LAMP-1 accumulation than (C) ManLAM bead phagosomes. (D) A synchronized phagocytosis assay was performed for 60 min. After fixation, MDMs were processed for immunohistochemical TEM. The distribution of LAMP-1 staining is shown as the percentage of LAMP-1–positive phagosomes containing washed, HSA, or ManLAM beads (mean ± SEM, $n = 2$). (E) HSA bead phagosomes show a higher degree of LAMP-1 colocalization than ManLAM bead phagosomes in macrophages following phagocytosis. MDM monolayers were incubated with either HSA or ManLAM fluorescent beads for 2 h. After washing, monolayers were fixed, permeabilized, and incubated with mouse anti–human LAMP-1 mAb followed by goat anti–mouse IgG secondary antibody. LAMP-1 colocalization was enumerated by confocal microscopy. Compartments that stain positive for LAMP-1 are red, beads in unfused phagosomes are green, and beads in fused phagolysosomes are yellow. The photomicrographs are from one representative experiment ($n = 3$).

M.tb strain Erdman) or control microspheres (beads) (washed or sham-treated [i.e., human serum albumin (HSA)-coated]) were added to monocyte-derived macrophages (MDMs) in a synchronized phagocytosis assay, and P-L fusion was assessed via quantitative transmission electron microscopy (TEM) using peroxidase as a lysosomal marker. Fig. 1, A–E shows photomicrographs of the TEM assay used showing the appearance of lysosomes and the P-L fusion patterns seen with the different beads.

P-L fusion for washed and HSA beads was 67.9 ± 3.0% and 36.2 ± 4.5%, respectively, after 60 min (Fig. 1 F). Thus, HSA precoating had a reproducible effect on P-L fusion and was an important control to include in our studies. In contrast to the control beads, P-L fusion for ManLAM beads was significantly reduced to 7.0 ± 1.3% ($n = 2$, $P < 0.005$ relative to both control groups) (Fig. 1 F). To further support our finding that phagosomes containing ManLAM beads exhibit limited P-L fusion, we quantified the amount of immunogold staining for the lysosome-associated membrane glycoprotein (LAMP-1) in bead phagosomes using TEM immunohistochemistry after synchronized phagocytosis (Fig. 2, A–C). Control bead phagosomes stained intensely for LAMP-1 (Fig. 2, A and B). In contrast, ManLAM bead phagosomes exhibited considerably reduced LAMP-1 staining (Fig. 2 C). The quantification and distribution of LAMP-1-positive phagosomes, indicative of P-L fusion events, are shown in Fig. 2 D. Relative to control beads, ManLAM bead phagosomes demonstrated a higher percent-

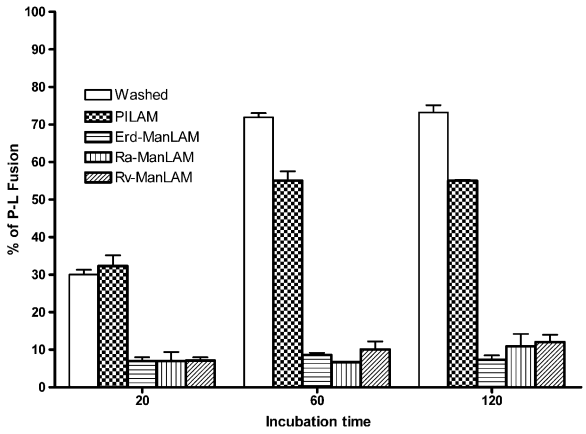

Figure 3. ManLAM from *M.tb* strains but not PILAM from *M. smegmatis* limits P-L fusion in macrophages. Washed, PILAM-, Ra-ManLAM-, Rv-ManLAM-, and Erd-ManLAM-coated beads were incubated with MDMs for the indicated times in the synchronized phagocytosis assay. The extent of P-L fusion of bead phagosomes was examined and enumerated via TEM as described in Fig. 1 F (mean ± SEM, $n = 2$).

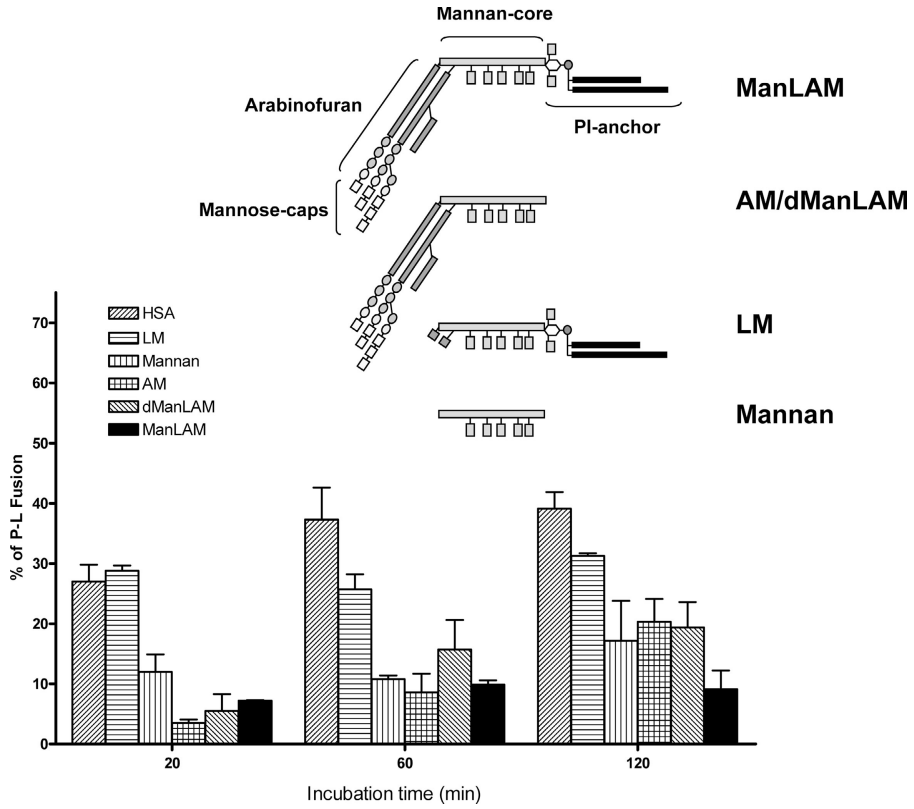

Figure 4. The terminal mannosyl caps of ManLAM are important in limiting P-L fusion. Beads coated with HSA, intact ManLAM or its substructures LM, mannan, arabinomannan, and dManLAM were used with MDMs in the synchronized phagocytosis assay for the indicated times. P-L fusion was examined and enumerated via TEM as in Fig. 1 F (mean ± SEM, $n = 2$).

age of weak staining (low number of gold particles/phagosome). As the number of gold particles/phagosome increased, these relative percentages shifted such that with strong staining (especially ≥24 gold particles/phagosome), there was a much higher percentage of control bead phagosomes relative to ManLAM bead phagosomes.

We next used confocal microscopy to assess P-L fusion as a complementary approach to the TEM studies. Green fluorescent beads were coated with or without ManLAM and added to MDM monolayers in the synchronized phagocytosis assay. The cells were fixed, immunostained, and analyzed for colocalization of bead phagosomes with LAMP-1 (Fig. 2 E). Consistent with the TEM studies, P-L fusion for washed and HSA beads was 61 ± 6% and 39 ± 3%, respectively. In contrast, P-L fusion for ManLAM beads was reduced to 19 ± 3% ($n = 3$, $P < 0.005$ relative to both control groups).

To compare the degree of P-L fusion by ManLAMs from different *M.tb* strains, we used in the TEM assay beads coated with ManLAMs from the *M.tb* virulent strains Erdman (Erd-ManLAM) and $H_{37}R_v$ (Rv-ManLAM), and the attenuated strain $H_{37}R_a$ (Ra-ManLAM). As above, Erd-ManLAM beads demonstrated limited P-L fusion (7.7 ± 1.2%) compared with the control beads (73.2 ± 1.9%) at 120 min (Fig. 3). The reduction in P-L fusion was equivalent for the Rv- and Ra-ManLAM beads (12.0 ± 2.0% and 10.9 ± 3.3%, respectively) at this time point. These results demonstrate that ManLAM-mediated phagocytosis by human macrophages leads to limited P-L fusion.

The terminal mannose caps of ManLAM are important in limiting P-L fusion in human macrophages

We used PILAM from *M. smegmatis* to assess whether the mannose capping found in ManLAM is important in limiting P-L fusion. In contrast to the results with ManLAM, P-L fusion for PILAM beads was comparable to that of control beads (55.0 ± 0.3%) after 120 min (Fig. 3). Thus the mannose caps of ManLAM appeared to be important in limiting P-L fusion. This result provided the first clue for involvement of the macrophage MR in this process. To further identify the domains of ManLAM that are important in limiting P-L fusion, we coated beads with deacylated ManLAM (dManLAM), lipomannan (LM), arabinomannan, and mannan, as well as with intact ManLAM from *M.tb*. P-L fusion was assessed in the TEM assay for periods up to 120 min (Fig. 4). Phagosomes containing LM-coated beads limited fusion to a small extent, whereas phagosomes containing mannan-, arabinomannan-, and dManLAM-coated beads limited fusion with lysosomes to a similar degree as for ManLAM bead phagosomes up to 60 min (Fig. 4). Thus, the ter-

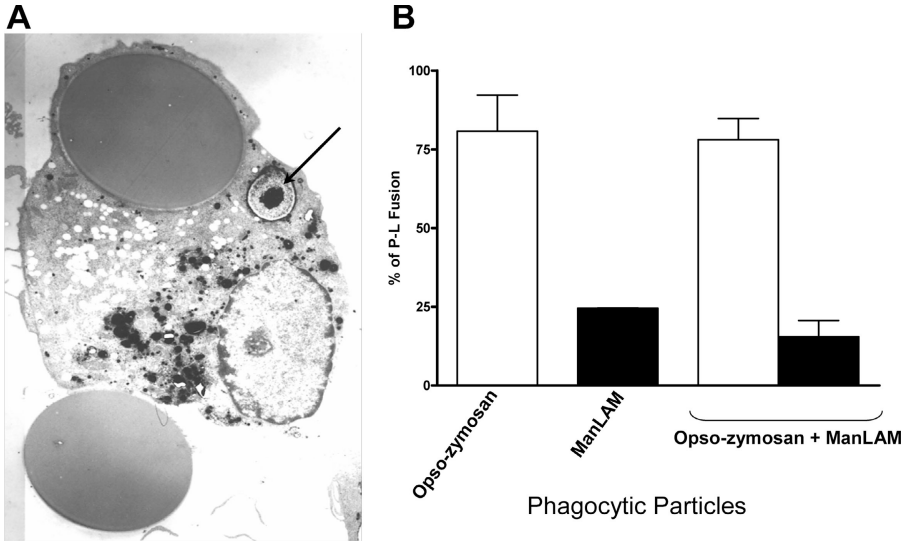

Figure 5. Limited P-L fusion is restricted to the ManLAM bead phagosome. MDM monolayers were incubated with ManLAM beads (20 μm) for 1 h followed by the addition of opsonized zymosan for 1 h before fixation. P-L fusion was analyzed by TEM as in Fig. 1. (A) Electron micrograph (×10,000) shows one unfused ManLAM bead phagosome along with an opsonized zymosan particle in a phagolysosome (arrow). A second ManLAM miscrosphere (shown at the bottom surface of the cell) is forming a phagocytic cup on the cell membrane. (B) The bar graph shows that the levels of P-L fusion for either opsonized zymosan or ManLAM beads phagocytosed individually by MDMs do not change when both types of particles are phagocytosed by the same cell. Shown is a representative experiment ($n = 3$).

minal mannose cap structures and branching arabinofurans are important in limiting P-L fusion. Beads coated with intact ManLAM continued to exhibit limited fusion at 120 min, whereas the inhibition of P-L fusion observed with the subcomponents of ManLAM began to reverse over this period (Fig. 4). This result suggests that both the fatty acids and terminal mannose caps of ManLAM are important in maintaining limited P-L fusion over time.

Limited P-L fusion is restricted to the ManLAM bead phagosome

In considering the potential mechanisms for the limited P-L fusion observed with the ManLAM beads, we next examined whether phagocytosis of these beads resulted in a global decrease in P-L fusion events in the macrophage. We used serum-opsonized zymosan as a phagocytic particle that is ingested via complement receptors and Fcγ receptors and undergoes P-L fusion (26). We incubated MDMs with ManLAM beads and opsonized zymosan particles individually or in combination and assessed P-L fusion events up to 120 min (Fig. 5). Opsonized zymosan particles were found fused in phagolysosomes with varying degrees of degradation. In coinfections, ManLAM bead phagosomes without lysosomal fusion were found in cells that also contained opsonized zymosan particles in phagolysosomes (Fig. 5 A). The overall levels of P-L fusion were not changed significantly for particles when used alone versus in combination (opsonized zymosan, 80.7 ± 11.5% vs. 78.1 ± 6.7%; ManLAM beads, 24.1 ± 0.1% vs. 15.5 ± 5.1%; P value not significant) (Fig. 5 B). For these experiments, we used ManLAM beads of different sizes, both smaller and larger than the 5- to 8-μm-sized opsonized zymosan particles. Equivalent results were produced in all cases. Thus, the decrease in P-L fusion is specific to the ManLAM bead phagosome.

The macrophage MR plays an important role in regulating P-L fusion of ManLAM beads

Specific phagocyte receptors direct the trafficking of newly formed phagosomes following phagocytosis (11). Because the MR is the principal receptor on human macrophages for ManLAM (27), we investigated whether the MR plays a role in limiting the degree of P-L fusion for ManLAM beads by using several complementary approaches. First, we performed a P-L fusion assay using human monocytes, which do not express functional MR (28), and consequently phagocytose less ManLAM beads comparable to control beads (27). The degree of P-L fusion for phagosomes containing HSA or ManLAM beads was equivalent in monocytes (33.6 ± 2.8% vs. 32.4 ± 2.1%, respectively; $n = 2$). In the second approach, HSA or ManLAM beads were added to MDMs in the presence or absence of mannan, a competitive blocker of the MR (14). Mannan did not influence the degree of P-L fusion for HSA beads (Fig. 6 A). In contrast, the low level of P-L fusion seen with ManLAM beads (10.5 ± 0.3%) was reversed with mannan (29.8 ± 2.4%; $n = 2$, $P < 0.005$) to a level comparable to HSA beads (31.9 ± 2.8%).

As a complementary third approach, we preincubated MDM monolayers with anti-MR mAb to block MR activity more specifically before adding ManLAM beads for the P-L fusion assay (Fig. 6 B). Both IgG_1 mAb preincubated monolayers and HSA beads were used as controls. P-L fusion of

HSA beads added to macrophages pretreated with IgG_1 or anti-MR mAb was 44.7 ± 1.35% and 48.3 ± 1.7%, respectively. ManLAM beads incubated with macrophages pretreated with IgG_1 demonstrated limited P-L fusion (18.5 ± 0.2%; $n = 2$, $P < 0.001$ when compared with the HSA bead groups). In contrast, when ManLAM beads were added to macrophages pretreated with anti-MR mAb, the limited degree of P-L fusion reversed completely to control levels (46.6 ± 2.6%) (Fig. 6 B). As expected, the total number of ManLAM beads associated with anti-MR mAb-treated macrophages was less than with the control IgG_1-treated macrophages.

In the fourth approach, we precoated ManLAM beads with the anti-LAM mAbs CS-35 or CS-40 (29, 30) (or preincubated them with IgG subtype control) to both mask the mannose caps and also redirect phagocytosis via Fcγ receptors that promote P-L fusion. ManLAM beads treated with CS-35 or CS-40 demonstrated high degrees of P-L fusion (70.0 ± 3.5% and 74.6 ± 0.4%, respectively) as opposed to the level of P-L fusion for ManLAM beads preincubated with no Ab or IgG subtype control (26.6 ± 4.5% and 33.4 ± 0.5%, respectively; $n = 2$, $P < 0.0005$ relative to the CS-35 and CS-40 groups) (Fig. 6 C).

The above experiments with macrophages provided evidence that engagement of the MR is necessary to limit P-L fusion of ManLAM beads following phagocytosis. We next examined whether the MR is sufficient in limiting P-L fusion

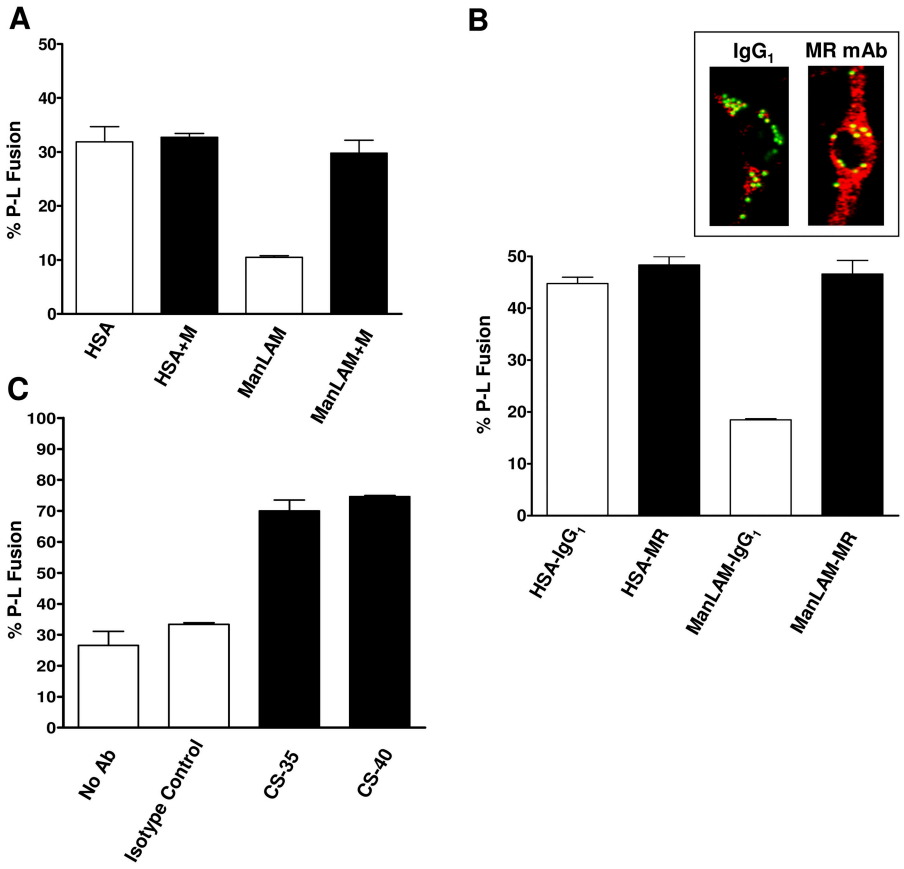

Figure 6. MR blockade with mannan or anti-MR antibody and redirected entry via FcγRs reverse the inhibition of P-L fusion of ManLAM beads in macrophages to control levels. (A) MDMs were preincubated with or without mannan for 30 min before adding HSA or ManLAM beads and allowing for synchronized phagocytosis over 60 min. P-L fusion was examined and enumerated by TEM as in Fig. 1 F (mean ± SEM, $n = 2$) and was significantly reduced with untreated ManLAM beads compared with the HSA control and mannan-treated bead groups ($P < 0.005$, one-way ANOVA). (B) MDMs were preincubated with anti-MR or control IgG_1 mAbs (10 μg/ml) for 20 min at 37°C followed by the addition of either HSA or ManLAM beads (MOI 100–200:1), and phagocytosis assay was then performed for 2 h. The cells were fixed, permeabilized, blocked, and then stained with anti-CD63 mAb followed by Alexa Fluor 647-conjugated mouse IgG. P-L fusion was examined and enumerated by confocal microscopy (mean ± SEM, $n = 2$). Data were analyzed via one-way ANOVA comparing the value of the ManLAM bead group (IgG_1 mAb-treated MDMs) with those of the HSA bead control groups and the ManLAM bead group (MR mAb-treated MDMs) ($P < 0.001$). Inset: A control IgG_1 mAb-treated MDM shows limited P-L fusion (left panel) and an anti-MR mAb-treated MDM shows increased P-L fusion (right panel) of ManLAM bead phagosomes. CD63-positive compartments are red, beads in unfused phagosomes are green, and those colocalized with CD63 are yellow. (C) ManLAM beads were preincubated with anti-LAM mAbs CS-35 or CS-40, IgG subtype control, or no mAb at 37°C for 60 min, washed, and added to MDM monolayers for the synchronized phagocytosis assay (60 min). P-L fusion was examined and quantified via TEM as in Fig. 1 F (mean ± SEM, $n = 2$) and was significantly increased in the groups treated with either CS-35 or CS-40 compared with each control group ($P < 0.0005$, one-way ANOVA).

by using a stable transfectant of the COS-1 cell expressing full-length MR (COS1-MR). This nonphagocytic fibroblast cell line has been used successfully as a model for phagocytosis of yeast cells mediated by the human macrophage MR (31) and for examining postphagocytic trafficking events of zymosan particles mediated by FcγRIIA (32). COS1-WT or COS1-MR monolayers were incubated with ManLAM beads in synchronized phagocytosis and P-L fusion assays. Cells were stained with the endosomal–lysosomal marker CD63 or LAMP-2 and analyzed for P-L fusion via confocal microscopy (Fig. 7). The total number of beads associated with COS1-WT and COS1-MR was 720 ± 26 and 1,424 ± 39 per 50 cells in each case, respectively (n = 2). However, results showed a higher level of P-L fusion for ManLAM beads in COS1-WT cells (mean % P-L fusion at a multiplicity of infection [MOI] of 100:1 = 13.3 ± 1.6%, n = 2, using CD63 or LAMP-2 antibodies) than in COS1-MR cells (mean % P-L fusion at an MOI of 100:1 = 6.0 ± 0.4%, n = 2, using CD63 or LAMP-2 antibodies) (Fig. 7, A and B). This represented a 55 ± 4% reduction in P-L fusion using the COS1-MR cells. As additional controls, we used HSA beads with COS1-WT and COS1-MR, which showed 12.1 ± 0.9% and 10.4 ± 1.1% P-L fusion (n =2), respectively, under the same conditions. The reduction in P-L fusion was consistent in assays using ManLAM beads at two different MOIs (100:1 and 20:1) and both CD63 and LAMP-2 mAbs (Fig. 7 B). Thus expression of the MR in a heterologous cell line caused a reduction in P-L fusion of ManLAM beads.

In a separate set of experiments, we analyzed the degree of P-L fusion for ManLAM beads mediated by the C-type lectin, DC-SIGN, using DC-SIGN-expressing COS-1 cells. The total number of beads associated with COS1-WT, COS1-MR, and COS1-DC-SIGN in this set of experiments was 512 ± 20, 1,102 ± 35, and 1,150 ± 24 per 50 cells in each case, respectively (n = 2). We found a comparable level of P-L fusion for ManLAM beads between COS1-WT and COS1-DC-SIGN cells (11.5 ± 2.8% vs. 9.5 ± 2.2% mean % P-L fusion at an MOI of 100:1 using CD63 or LAMP-2 antibodies; n = 2), as opposed to the low level of P-L fusion with COS1-MR cells (3.2 ± 0.5% using CD63 or LAMP-2 antibodies; n = 2), indicating that, unlike the MR, entry via DC-SIGN is not associated with reduced P-L fusion.

A

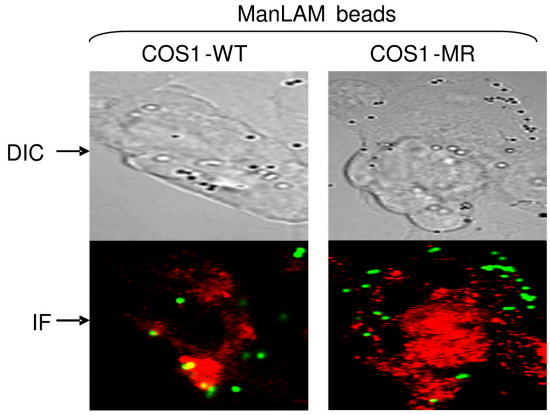

B

MOI	Late Endosome/ Lysosomal Marker	% P-L Fusion		% Reduction in P-L Fusion*
		ManLAM beads COS1-WT	ManLAM beads COS1-MR	
100:1	CD63	14.8	6.2	**58**
	LAMP-2	11.7	5.7	**51**
20:1	CD63	8.6	3.5	**59**
	LAMP-2	6.5	2.5	**61**

*Reduction in P-L Fusion Relative to COS1-WT

Figure 7. ManLAM beads demonstrate reduced P-L fusion in MR-expressing COS-1 cells. COS1-WT and COS1-MR cells adhered to glass coverslips were incubated with ManLAM beads (MOI 20:1 or 100:1) for 3 h using a synchronized phagocytosis assay. Cell monolayers were fixed, permeabilized, and stained with anti-human CD63 or LAMP-2 mAbs followed by Alexa Fluor 647-conjugated goat anti-mouse IgG. P-L fusion was examined and enumerated via confocal microscopy. (A) Phase and fluorescence microscopy images of ManLAM beads in COS1-WT and COS1-MR cells. CD63 positive compartments are red, beads in unfused phagosomes are green, and those colocalized with CD63 are yellow. Shown is a representative experiment (n = 2). DIC, differential interference contrast; IF, immunofluorescence. (B) Percent P-L fusion of ManLAM beads using two different MOIs (100:1 and 20:1, n = 2, performed in duplicate).

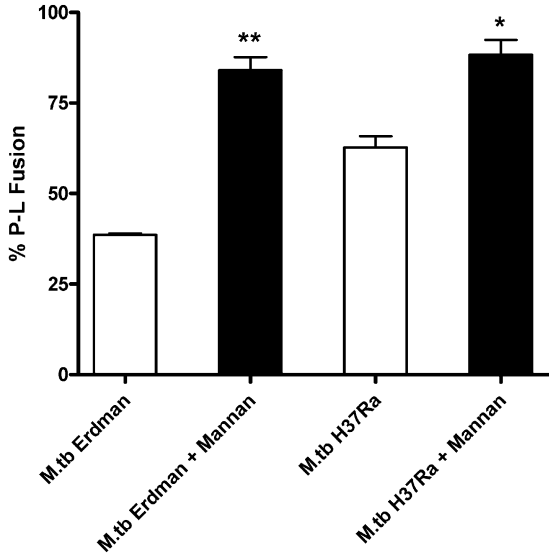

Figure 8. MR blockade increases the level of P-L fusion of phagosomes containing live *M.tb* bacilli following phagocytosis. MDMs were preincubated with or without mannan at 37°C for 30 min followed by incubation with the live *M.tb* strains Erdman and $H_{37}R_a$ (MOI of 6.25 bacilli per MDM) for 2 h. P-L fusion was examined and quantified via TEM as in Figure 1 F (mean ± SEM, $n = 2$). **$P < 0.01$ (Erdman) and *$P < 0.05$ ($H_{37}R_a$) relative to the no mannan condition for each strain.

As a final approach, we evaluated the degree of P-L fusion in human macrophages for phagosomes containing live *M.tb* strains Erdman or $H_{37}R_a$ in the presence or absence of mannan during phagocytosis (Fig. 8). As previously shown, phagocytosis of *M.tb* Erdman is mediated by the MR and complement receptors, and phagocytosis of *M.tb* $H_{37}R_a$ occurs primarily via complement receptors (14). Our results showed that for phagosomes containing live *M.tb* Erdman, the degree of P-L fusion with or without mannan was 84.0 ± 5.1% and 38.6 ± 0.6%, respectively, whereas for phagosomes containing *M.tb* $H_{37}R_a$ the degree of P-L fusion with or without mannan was 88.3 ± 5.8% and 62.7 ± 4.4%, respectively (Fig. 8). Thus, similar to the results with ManLAM beads, blockade of the MR during phagocytosis of *M.tb* led to a reversal of the limited P-L fusion normally seen. The basal level of P-L fusion for the attenuated $H_{37}R_a$ strain was higher than that seen with the virulent Erdman strain; however, in both cases an increase in P-L fusion was observed with MR blockade.

Heat-killed and γ-irradiated *M.tb* have markedly altered cell wall morphology and reduced amounts of ManLAM on the surface

In contrast with live mycobacteria, the phagosome of heat-killed *M.tb* fuses at a higher rate with lysosomes (33, 34). Because ManLAM is a lipoglycan, it is presumed to be resistant to heating, and heat-killed mycobacteria could be predicted to have unaltered ManLAM on their surface. However, no data exist on the nature of the cell wall of heat-killed mycobacteria. The process of killing *M.tb* at 80–90°C is harsh, with the potential to markedly alter the cell wall and release or modify ManLAM on its cell surface. To examine this possibility, we used immunogold TEM with the anti-LAM mAbs CS-35 and CS-40 to localize ManLAM on the *M.tb* cell surface (Fig. 9). A significant number of live *M.tb* that were directly fixed in paraformaldehyde demonstrated an intact cell wall architecture with intense staining for ManLAM (Fig. 9, A, B, D, and E). In contrast, only ∼25% of heat-killed bacilli demonstrated an intact cell wall architecture (relative to live *M.tb*) and these bacilli had significantly less ManLAM on their surface (Fig. 9, C–E). Further, our studies revealed that γ-irradiated *M.tb* are essentially devoid of an intact cell wall architecture and more distorted than heat-killed bacilli, and have little ManLAM on their surface (Fig. 9, D and E). These studies make the important observation that heat-killing and γ-irradiation are very destructive procedures for the mycobacterial cell wall structure and lead to ManLAM being released. The loss of ManLAM likely limits the ability of bacilli to interact with the MR during phagocytosis.

DISCUSSION

Macrophage PRRs recognize a variety of microbial surface determinants and bridge innate and adaptive immune responses by regulating endosomal and phagosomal traffic as well as pro- and anti-inflammatory cytokine production. Although much attention has recently focused on the ability of *M.tb* ManLAM to regulate phagosome biogenesis, the role of specific macrophage PRRs in directing this process has not been clear. Here we provide several lines of evidence to demonstrate that engagement of the MR by *M.tb* ManLAM directs phagocytic particles and live *M.tb* bacilli to a phagosomal compartment that has limited fusion with lysosomes. This process is specific for the MR and ManLAM, because entry of ManLAM via another C-type lectin PRR, DC-SIGN, does not mediate this effect, nor does PILAM or LM. Also, monocytes that do not express the MR are not capable of limiting P-L fusion. Furthermore, limited P-L fusion can be reversed by masking the mannose caps of ManLAM and redirecting ManLAM entry through other phagocytic receptors such as FcγRs. The MR is sufficient in limiting P-L fusion as evidenced by experiments using COS1-MR cells where the reduction in P-L fusion (>50%) was comparable to that seen with human macrophages. Such an event was specific to the ManLAM-containing phagosome rather than due to a global effect of ManLAM on vesicle trafficking in the cell. Most compelling, our data provide the first evidence that MR blockade on human macrophages results in increased P-L fusion of live *M.tb* following phagocytosis (Fig. 8).

This work lends support to a two-step model for *M.tb* phagosome biogenesis. In step 1, recognition of *M.tb* surface determinants by specific receptors leads to receptor-mediated signaling, actin cytoskeleton reorganization, and directed entry into the nascent phagosome. Evidence for such a step comes from numerous studies demonstrating the rapidity with which microbial engulfment occurs, the phago-

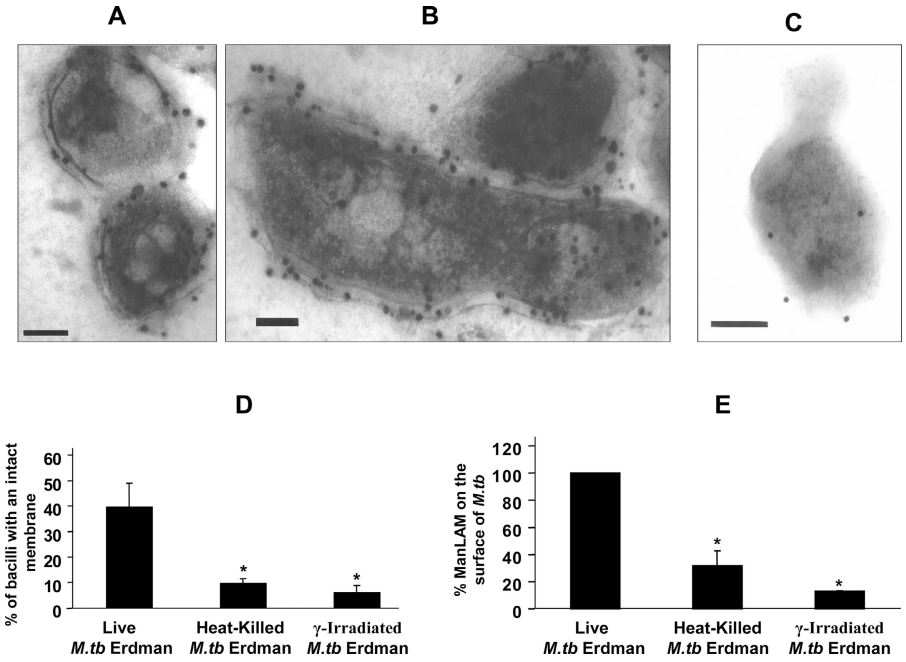

Figure 9. Heat-killing and γ-irradiation of *M.tb* alter the integrity of the bacterial cell wall and decrease the amount of surface-exposed ManLAM. Single suspensions of plate-grown *M.tb* strain Erdman were kept alive or were killed by heating or γ-irradiation. Bacilli were fixed with 2% paraformaldehyde, washed, embedded in LR White, thin sectioned, and immunostained with anti-LAM mAb CS-35 or CS-40 followed by 10 nm immunogold-conjugated goat anti–mouse secondary antibody before viewing by TEM. Electron micrographs of (A) live *M.tb* stained with CS-35 (bar, 100 nm), (B) live *M.tb* stained with CS-40 (bar, 100 nm), or (C) heat-killed *M.tb* stained with CS-35 (bar, 100 nm). (D) Graph shows percentage of bacilli in the indicated groups that have an intact cell wall architecture. (E) Graph shows amount of ManLAM exposed on the surface of live, heat-killed, and γ-irradiated *M.tb*. Results are shown as a percentage of immunogold particles/*M.tb* bacillus relative to control live *M.tb* set at 100% (*$P < 0.05$).

some is generated and fusion and fission events within the endolysosomal pathway proceed (<30 min) (11). That limited P-L fusion can be reversed by redirecting ManLAM and *M.tb* bacilli to alternative phagocytic pathways emphasizes the importance of this step. In step 2, the unique *M.tb* phagosome is maintained over hours to days. Here *M.tb* viability is particularly critical, and several bacterial-derived processes are active in blocking phagosome maturation (6).

Recent studies provide convincing evidence that ManLAM blocks phagosome maturation in murine macrophages and a human monocytic cell line (9, 10). Our present study is consistent with these observations and extends them to primary human macrophages. We demonstrate for the first time the importance of the MR in this process with both ManLAM and live virulent *M.tb*. The published work using the murine macrophage cell line J774 (10) did not examine the contribution of the MR, reported to be expressed by these cells (35).

The MR is a type I transmembrane glycoprotein and member of the C-type lectin family that binds mannose and fucose with highest affinity (36). Detailed studies on trafficking of the MR have focused primarily on pinocytosis using mannosylated proteins (37). Macrophages contain large intracellular pools of MR within early endosomes, which undergo continual rapid recycling to the cell surface (37). The intracellular compartment containing macroparticles (>1 μm) phagocytosed by the MR has not been well characterized.

Little is known regarding MR-specific signaling and trafficking pathways. However, the literature provides clues to the potential mechanisms whereby the MR may regulate phagosomal traffic. MR expression/function is increased by IL-4 and IL-13 (38–40) and is inhibited by IFNγ. IL-4 and IL-13 decrease, whereas IFNγ increases particle sorting to lysosomes (39). Enhanced MR endocytic activity by IL-4 and IL-13 involves activation of phosphatidylinositol 3 kinases (39) that are critically involved in cytoskeletal organization. Thus these data suggest that the MR may preferentially sort phagocytosed particles to nonlysosomal compartments. Relevant to *M.tb* pathogenesis, IL-4 and IL-13 produce an alternative activation state of macrophages [reviewed in (41)] that may enhance intracellular survival of microbes. Alveolar macrophages are a prototypic alternatively activated cell with high MR activity.

Our studies show that both the MR and DC-SIGN recognize ManLAM, but regulate phagosomal trafficking differently, where DC-SIGN directs phagocytic particles to the phagolysosome. Several studies have reported that DC-SIGN and its homologues L-SIGN and SIGNR1 target ManLAM and/or mycobacteria to lysosomes in dendritic cells (17, 42, 43). This observation is supported by the fact that the cytoplasmic tail of DC-SIGN possesses the "tri-acidic cluster and di-leucine" signaling motifs that target endocytosed molecules to lysosomes and MHC class II–positive late endosomes (44).

The MR lacks such motifs and has only one immunoreceptor tyrosin-based activation motif–like cytoplasmic motif containing Tyr[18] (a member of a diaromatic amino acid sequence), which is involved in efficient phagocytosis and endocytosis (45, 46) and endosomal sorting (46). Thus these studies, along with the data in the current work, raise the possibility that the trafficking fate of *M.tb* bacilli and ManLAM in a given cell following phagocytosis will depend on the relative amount and activity of the MR and DC-SIGN on the cell surface. Because macrophages express high MR and DCs express high DC-SIGN activities, we speculate that this difference may provide one explanation for why macrophages serve as the major intracellular niche for *M.tb* rather than DCs, which are more potent in processing endocytosed products in lysosomes. Published literature and our own unpublished data provide evidence for little or no DC-SIGN expression on MDMs (47).

Beyond these observations, ligation of the MR by ManLAM has been linked to the generation of an anti-inflammatory cytokine program on monocyte-derived DCs (19, 21) and, in one study, to calcium responses in MDMs (48). The latter is of interest given that maturation arrest of the *M.tb* phagosome has been linked to a block in the increase of cytosolic calcium during phagocytosis of live virulent *M.tb* by human macrophages. This is due to a defect in signaling by Ca^{2+}/calmodulin-dependent protein kinase II and sphingosine kinase (49, 50). Thus it is possible that ligation of the MR by ManLAM generates a negative signal for P-L fusion events in the host cell, a hypothesis we are currently exploring.

We have previously determined that the MR is involved in phagocytosis of the virulent *M.tb* strains Erdman and $H_{37}R_v$ but not the attenuated strain $H_{37}R_a$ by MDMs (14). However, when ManLAMs purified from these strains were studied for MR involvement in phagocytosis using the bead model, we found that all three ManLAM types are recognized by the MR, but to a different extent (Erd-ManLAM > Rv-ManLAM > Ra-ManLAM) (51). In the current study, all three purified ManLAMs limited P-L fusion to a similar extent. However, a different picture emerged when live bacilli were used. The high degree of P-L fusion observed in the presence of mannan for the *M.tb* $H_{37}R_a$ strain was similar to that of the *M.tb* Erdman strain; however, the basal level of P-L fusion in the absence of mannan was significantly higher for the *M.tb* $H_{37}R_a$ strain (Fig. 8), as was observed in an early study (52). Taken together, our data suggest that there is only a very small interaction of the live *M.tb* $H_{37}R_a$ strain with the MR during phagocytosis by MDMs that is difficult to detect in tissue culture and that this limited interaction results in a higher degree of P-L fusion during phagocytosis. There is accumulating evidence that the precise nature of the mannose caps of ManLAM and their presentation may impact recognition by the MR and consequently the host response.

Our study provides new insight into the structural domains of ManLAM that are important in the limiting of P-L fusion. It is clear that the mannose caps of ManLAM play a key role in this process by binding to the carbohydrate recognition domains of the MR. We hypothesize that the branching arabinofurans of ManLAM play an important role in properly orienting the mannose caps for recognition by the MR. LM limited P-L fusion poorly (Fig. 4), consistent with its inability to bind to the MR (15), which is likely due to the nature of its mannan linkages (53) in the presence of the lipid tail. Our data provide evidence that both the glycosyl phosphatidyl-1-*myo*-inositol anchor and carbohydrates of ManLAM are important in limiting P-L fusion over time, because the limited P-L fusion seen with mannan, arabinomannan, and dManLAM was reversed between 2 and 6 h. The ability of the glycosyl phosphatidyl-1-*myo*-inositol anchor to intercalate into the plasma membrane of mammalian cells (54) may be important in limiting P-L fusion over time.

Our studies on heat-killed and γ-irradiated *M.tb* provide evidence that the surface-exposed molecules of these bacilli are globally altered and as such would be expected to interact with the macrophage very differently from live mycobacteria. This concept is supported by a recent study that described a difference between live and dead bacilli with regard to P-L fusion related to a heat-sensitive secreted *M.tb* lipid phosphatase (34). These data, together with our finding that live bacilli retain greater amounts of ManLAM on their surface than killed bacilli, highlight the importance of an intact mycobacterial cell wall architecture in early microbe–host interactions. The presence of ManLAM on the surface of live bacilli enhances their interaction with the MR and MR-mediated trafficking pathways.

Relevance of the MR to tuberculosis is highlighted by recent human genetic studies that show a major locus for susceptibility to mycobacterial infection on chromosome 10p13, mapped to the location of the MR gene (55, 56). Our accumulated data from this and previous studies strongly support the notion that the MR-ManLAM pathway initiates the development of a safe intracellular niche for *M.tb* following phagocytosis and thus plays an important role in the pathogenesis of tuberculosis.

In this study, we add an important missing piece to the growing body of evidence that ManLAM regulates *M.tb* phagosome biogenesis. We demonstrate that engagement of the MR on human macrophages by *M.tb* ManLAM initiates a specific phagocytic pathway that results in limited P-L fusion. Because the alveolar macrophage has relatively high MR activity, we reason that use of the MR-ManLAM pathway may be particularly important in the outcome of primary infection in the lung, where the number of *M.tb* bacilli encountering this cell is believed to be very low.

MATERIALS AND METHODS

Antigens and antibodies. Rv-ManLAM, dManLAM, *M.tb* LM, PILAM from *M. smegmatis,* and CS-35 and CS-40 mAbs were provided by John T. Belisle (Colorado State University, Fort Collins, CO; NIH-NIAID contract NO1 AI-75320). Erd-ManLAM and Ra-ManLAM were purified as described previously (51). For experiments with COS-1 cells, Rv-ManLAM from plate-grown *M.tb* $H_{37}R_v$ was purified as described previously (57). *M.tb* $H_{37}R_v$ arabinomannan and mannan were kindly provided by Mamadow Daffe (Institut de Pharmacologie et Biologie Structurale, Toulouse,

France) (58). Anti–human LAMP-1 (H4A3) and LAMP-2 (H4B4) mAbs were purchased from the University of Iowa Hybridoma Bank. Anti–human CD63 (for immunofluorescence) and CD206 (for flow cytometry) mAbs were purchased from BD Biosciences. For receptor blocking, CD206 (MR) mAb was purchased from Serotech. Ultra-small immunogold conjugate antibody was obtained from AURION and labeled goat anti–mouse IgG was obtained from Invitrogen.

Monocyte-derived macrophages. PBMCs were isolated from healthy donors (using an approved protocol by The Ohio State University Institutional Review Board) and day 1 monocytes or day 5 MDMs cultivated as described previously (27). Monolayers in 24-well tissue culture plates contained approximately 1.5–2.0 × 10^5 monocytes or MDMs.

Preparation of *M.tb* cell suspensions and washed, HSA-coated, and lipoglycan-coated polystyrene beads. Single suspensions of *M.tb* for P-L fusion assays were prepared using 9–12 d plate-grown bacilli as described (14). HSA- (sham control), ManLAM-, PILAM-, LM-, dManLAM-, mannan-, and arabinomannan-coated beads were prepared as previously described previously (15) using Polybead polystyrene beads (1, 6, or 20 μm in diameter) (Polysciences). Beads were finally adjusted to 4.0 × 10^8/ml in 0.5% HSA before use with MDMs or COS-1 cells. For washed beads, Polybead polystyrene beads were washed twice in 0.05 M carbonate-bicarbonate buffer before use.

Synchronized phagocytosis assay. Monocyte or MDM monolayers on coverslips were briefly (2 min) cooled to 4°C before adding the beads (4 × 10^7/well) at 4°C for 5 min to allow them to settle onto the surface of the monolayers; monolayers were subsequently warmed up to 37°C for various periods. For TEM assays of P-L fusion, monocyte or MDM monolayers were incubated with 1 mg/ml horseradish peroxidase (Sigma-Aldrich) in RPMI 1640-20 mM Hepes containing 1 mg/ml HSA (RHH medium) at 37°C for 2 h, washed and chased for 1 h in RHH medium before adding the beads (59).

Quantitative P-L fusion assay using TEM. After the synchronized phagocytosis assay using beads, cell monolayers were washed with prewarmed RPMI 1640 medium, fixed in 2.5% glutaraldehyde in 0.1 M sodium cacodylate buffer (pH 7.2) for 60 min, and washed three times in sodium cacodylate buffer. To reveal peroxidase, monolayers were then incubated at RT for 15 min in 0.05 M Tris-HCl buffer (pH 7.6) containing 1 mg/ml diaminobenzidine and 0.01% H_2O_2 followed by postfixation in 1% osmium tetroxide and an en bloc staining in 2.5% uranyl acetate. After dehydration in gradient ethanol solutions (15 min each in 50 and 70% ethanol, 30 min in 95%, and 60 min in 100% ethanol with 2 changes), monolayers were embedded in the mixture of Eponate 12 and ethanol (1:1) O/N. Two further incubations in 100% Eponate were performed before curing the samples at 70°C O/N. Thin sections were then cut at 100 nm and stained with 5% uranyl acetate and Reynold's lead citrate before viewing by TEM. For the P-L fusion assay using live *M.tb*, bacilli (1.25 × 10^6/well) were incubated with horseradish peroxidase–preloaded MDM monolayers at 37°C for 2 h, washed, sections prepared for TEM, and P-L fusion for single bacteria within phagosomes was quantified.

In certain TEM experiments, MDM monolayers were preincubated with or without mannan (4 mg/ml) at 37°C for 30 min before adding beads or live *M.tb* to the monolayers. In other experiments, beads were incubated with anti-LAM mAbs CS-35 or CS-40 or subtype control mAb (1:300 dilution each) at 37°C for 60 min and washed before addition to the MDM monolayers. Finally, in TEM experiments that used opsonized zymosan, particles were incubated in 50% human serum and washed. Opsonized zymosan particles were then added either alone or following a 60-min incubation with either HSA or ManLAM beads (1, 6, 10, or 20 μm in diameter) to MDM monolayers for an additional 60 min before fixation.

The percentage of bead, *M.tb*, or zymosan phagosomes that were fused with lysosomes in the horseradish peroxidase assay was quantified by counting >300 consecutive phagosomes in each test group in two independent experiments using two different donors.

For the TEM immunohistochemical assay, MDM monolayers were embedded in LR White and sections stained with a primary mAb against LAMP-1, and then an ultra-small (<1 nm) immunogold-conjugated goat anti–mouse antibody followed by silver enhancement. The number of immunogold particles was quantified by counting over 1,000 consecutive phagosomes in each test group in two independent experiments using two different donors.

Quantitative P-L fusion assay using confocal microscopy. Phagocytosis assays with beads were performed as above, except that green fluorescent beads (1 μm diameter; Polysciences) were used. Cell monolayers on coverslips were washed with PBS, fixed with 2% paraformaldehyde, and permeabilized with 100% methanol for 5 min at RT. The cells were blocked O/N at 4°C in blocking buffer (D-PBS + 5 mg/ml BSA + 10% heat-inactivated fetal bovine serum), stained with mAbs against late endosomal/lysosomal markers (LAMP-1, LAMP-2, or CD63; 0.5 μg/ml final concentration for each), and next stained with Alexa Fluor 647-conjugated goat anti–mouse IgG secondary antibody (4 μg/ml final concentration). After extensive washing in blocking buffer, the coverslips were dried, mounted on glass slides, and examined via confocal microscopy (LSM 510; Carl Zeiss MicroImaging, Inc.). In certain experiments, MDM monolayers were incubated with isotype control IgG_1 or anti-MR mAb at 37°C for 20 min before adding HSA or ManLAM green fluorescent beads to the monolayers for 2 h.

The percentage of bead phagosomes that colocalized with lysosomal markers was quantified by counting over 300 consecutive phagosomes in each test group in two or more independent experiments using a minimum of two different donors.

Creation of MR and DC-SIGN expression constructs and stable COS-1 cell lines. A 4817-bp cDNA, spanning the full-length MR-coding sequence and flanking regions, was obtained from IL-4 stimulated human MDM MRNA via reverse-transcriptase polymerase chain reaction using oligo-dT, M-MLV reverse transcriptase (Invitrogen), and sequence-specific primers. Initially, the fragment was cloned into pT7Blue vector (Novagen). To create an MR expression construct, a 4490-bp cDNA (MR sequence position 101–4591) (60) was amplified via polymerase chain reaction from the pT7Blue/MRcDNA clone by using *pfuUltra* High Fidelity DNA Polymerase (Stratagene) and MR-specific sense (5′-CACCGCCATGAGGCTACCCCTGCTCCTG-3′) and antisense (5′GGACAGACCAGTACAATTCAGTACTCA-3′) primers. The fragment was cloned into the mammalian expression vector pcDNA3.1/V5-His-TOPO using a pcDNA3.1 Directional TOPO Expression Kit (Invitrogen) according to the manufacturer's instructions. The MR expression construct, designated pcDNA3.1/V5-His-TOPO/4490-bp MR, was initially made in *Escherichia coli* TOP10 (supplied in the kit) but was finally propagated and stabilized at 30°C in a special-purpose *E. coli* Stbl2 strain (Invitrogen).

To make a DC-SIGN expression construct, a 1280-bp cDNA fragment was amplified via polymerase chain reaction from Human Placenta QUICK-Clone cDNA mix (BD Biosciences Clontech) using DC-SIGN–specific sense (5′-CGCGGATCCAGAGTGGGGTGACATGAGTGAC-3′) and antisense (5′-CGGAATTCAGGTCGAAGGATGGAGAGAAGG-3′) primers. The fragment was cloned into the unique BamHI and EcoRI sites (also added to the DC-SIGN primers, shown as underlined) of the mammalian expression vector pSecTag2 (Invitrogen) resulting in the DC-SIGN expression construct pSecTag2/DC-SIGN.

For construction of stable MR and DC-SIGN–expressing cell lines, plasmid DNA of the individual constructs was transfected into COS-1 cells (ATCC) using Lipofectamine 2000 Reagent (Invitrogen), according to the supplier's instructions. Transfected cells were initially selected in bulk with the antibiotic G418 for MR and zeocin for DC-SIGN clones (400 μg/ml in each case). The antibiotic-resistant clones of each type were pooled together, stained with either anti-MR (CD206) or anti-DC-SIGN (CD209,

R&D Systems) mAbs, and then subjected to sorting of positive cells into single clones in a 96-well format via fluorescent-activated cell sorting (FACSCalibur; Becton Dickinson). The single clones were further expanded and screened for stable expression of the MR or DC-SIGN via flow cytometry and Western blotting.

P-L fusion assay using COS-1 stable transfectants and ManLAM-coated fluorescent beads. Freshly grown COS1-WT, COS1-MR, or COS1-DC-SIGN cells were seeded onto coverslips (10^5 cells/well, triplicate wells/test group) in wells of a 24-well tissue culture plate and incubated O/N to form monolayers. Cell monolayers were washed and repleted with PBS-HHG medium (PBS + 10 mM Hepes + 1 mg/ml HSA + 0.1% glucose) to which HSA or ManLAM beads were added (MOIs of 20–100:1) followed by centrifugation of the culture plates at 4°C to pellet the beads onto the monolayers. The cells were further cooled at 4°C for 15 min before warming up to 37°C for 3 h to allow for the synchronized uptake of beads. After washing, the cells were fixed, permeabilized, stained with either CD63 or LAMP-2 mAb and then Alexa Fluor 647-conjugated secondary antibody. The monolayers were processed for confocal microscopy and analyzed as described above. The percentage of bead phagosomes that were colocalized with the late endosome/lysosome markers was enumerated by viewing 20 consecutive images (containing 1–5 cells/image) and counting at least 500 beads in each test group for each of the two mAbs, CD63 or LAMP-2, in two independent experiments.

TEM of live, heat-killed, and γ-irradiated *M.tb*. Single suspensions of plate-grown live *M.tb* strain Erdman were fixed in 2% paraformaldehyde and processed for TEM. The morphology of the bacterial surface and presence of ManLAM were compared with groups in which the bacteria were either heat-killed (at 80°C for 60 min) or γ-irradiated (2.5 MRad for 18 h) before fixation. Fixed bacteria were rinsed three times in cacodylate buffer and postfixed with 1% osmium tetroxide in 0.1 M cacodylate buffer with 1.5% potassium ferrocyanide for 1.5 h. After rinsing with buffer and distilled water, cells were stained with 2.5% uranyl acetate for 30 min. A stepwise prolonged dehydration procedure was followed that consisted of 50% acetone for 15 min, 70% acetone two times for 20 min each, 95% acetone three times for 20 min each, and absolute acetone four times for 1 h each. A 1:1 mixture of absolute acetone and propylene oxide for 1 h was then followed by two incubations in 100% propylene, the first for 45 min and the second for O/N. The samples were embedded in an increasing concentration of Spurr's resin (Polysciences) mixed with propylene oxide for 2 h. Two O/N incubations in 100% Spurr's resin were then performed before curing at 60°C for 48 h. Thin sections were cut at 100 nm, stained with either CS-35 or CS-40 anti-LAM mAb (1:10 dilution for each) followed by secondary goat anti–mouse 10 nm conjugate antibody, and viewed by TEM (Hitachi H-7000). The number of immunogold particles/*M.tb* bacillus was enumerated for 50 or more bacteria in each group.

We would like to thank the Central Microscopy Research Facility at the University of Iowa and the Campus Microscopy & Imaging Facility at the Ohio State University.

This work was supported in part by the National Institutes of Health (grant nos. AI052458 and AI33004) and a Department of Veterans Affairs Merit Review Award.

The authors have no conflicting financial interests.

Submitted: 21 June 2005
Accepted: 26 August 2005

REFERENCES

1. Fenton, M.J., L.W. Riley, and L.S. Schlesinger. 2005. Receptor-mediated recognition of *Mycobacterium tuberculosis* by host cells. *In* Tuberculosis and the Tubercle Bacillus. S.T. Cole, K.D. Eisenach, D.N. McMurray, and W.R. Jacobs, Jr., editors. ASM Press, New York. 405–426.
2. Brennan, P.J., and H. Nikaido. 1995. The envelope of mycobacteria. *Annu. Rev. Biochem.* 64:29–63.
3. Strohmeier, G.R., and M.J. Fenton. 1999. Roles of lipoarabinomannan in the pathogenesis of tuberculosis. *Microbes Infect.* 1:709–717.
4. Hunter, S.W., and P.J. Brennan. 1990. Evidence for the presence of a phosphatidylinositol anchor on the lipoarabinomannan and lipomannan of *Mycobacterium tuberculosis*. *J. Biol. Chem.* 265:9272–9279.
5. Armstrong, J.A., and P.D. Hart. 1971. Response of cultured macrophages to *Mycobacterium tuberculosis*, with observations on fusion of lysosomes with phagosomes. *J. Exp. Med.* 134:713–740.
6. Russell, D.G. 2001. *Mycobacterium tuberculosis*: here today, and here tomorrow. *Nat. Rev. Mol. Cell Biol.* 2:569–577.
7. Kusner, D.J. 2005. Mechanisms of mycobacterial persistence in tuberculosis. *Clin. Immunol.* 114:239–247.
8. Chua, J., I. Vergne, S. Master, and V. Deretic. 2004. A tale of two lipids: *Mycobacterium tuberculosis* phagosome maturation arrest. *Curr. Opin. Microbiol.* 7:71–77.
9. Hmama, Z., K. Sendide, A. Talal, R. Garcia, K. Dobos, and N.E. Reiner. 2004. Quantitative analysis of phagolysosome fusion in intact cells: inhibition by mycobacterial lipoarabinomannan and rescue by an 1alpha,25-dihydroxyvitamin D3-phosphoinositide 3-kinase pathway. *J. Cell Sci.* 117:2131–2140.
10. Fratti, R.A., J. Chua, I. Vergne, and V. Deretic. 2003. *Mycobacterium tuberculosis* glycosylated phosphatidylinositol causes phagosome maturation arrest. *Proc. Natl. Acad. Sci. USA.* 100:5437–5442.
11. Aderem, A., and D.M. Underhill. 1999. Mechanisms of phagocytosis in macrophages. *Annu. Rev. Immunol.* 17:593–623.
12. Janeway, C.A., Jr., and R. Medzhitov. 2002. Innate immune recognition. *Annu. Rev. Immunol.* 20:197–216.
13. McGreal, E.P., J.L. Miller, and S. Gordon. 2005. Ligand recognition by antigen-presenting cell C-type lectin receptors. *Curr. Opin. Immunol.* 17:18–24.
14. Schlesinger, L.S. 1993. Macrophage phagocytosis of virulent but not attenuated strains of *Mycobacterium tuberculosis* is mediated by mannose receptors in addition to complement receptors. *J. Immunol.* 150: 2920–2930.
15. Schlesinger, L.S., S.R. Hull, and T.M. Kaufman. 1994. Binding of the terminal mannosyl units of lipoarabinomannan from a virulent strain of *Mycobacterium tuberculosis* to human macrophages. *J. Immunol.* 152: 4070–4079.
16. Maeda, N., J. Nigou, J.L. Herrmann, M. Jackson, A. Amara, P.H. Lagrange, G. Puzo, B. Gicquel, and O. Neyrolles. 2003. The cell surface receptor DC-SIGN discriminates between *Mycobacterium* species through selective recognition of the mannose caps on lipoarabinomannan. *J. Biol. Chem.* 278:5513–5516.
17. Geijtenbeek, T.B., S.J. Van Vliet, E.A. Koppel, M. Sanchez-Hernandez, C.M. Vandenbroucke-Grauls, B. Appelmelk, and Y. van Kooyk. 2003. Mycobacteria target DC-SIGN to suppress dendritic cell function. *J. Exp. Med.* 197:7–17.
18. Means, T.K., E. Lien, A. Yoshimura, S. Wang, D.T. Golenbock, and M.J. Fenton. 1999. The CD14 ligands lipoarabinomannan and lipopolysaccharide differ in their requirement for toll-like receptors. *J. Immunol.* 163:6748–6755.
19. Chieppa, M., G. Bianchi, A. Doni, A. Del Prete, M. Sironi, G. Laskarin, P. Monti, L. Piemonti, A. Biondi, A. Mantovani, et al. 2003. Cross-linking of the mannose receptor on monocyte-derived dendritic cells activates an anti-inflammatory immunosuppressive program. *J. Immunol.* 171:4552–4560.
20. Astarie-Dequeker, C., E.N. N'Diaye, V. Le Cabec, M.G. Rittig, J. Prandi, and I. Maridonneau-Parini. 1999. The mannose receptor mediates uptake of pathogenic and nonpathogenic mycobacteria and bypasses bactericidal responses in human macrophages. *Infect. Immun.* 67: 469–477.
21. Nigou, J., C. Zelle-Rieser, M. Gilleron, M. Thurnher, and G. Puzo. 2001. Mannosylated liparabinomannans inhibit IL-12 production by human dendritic cells: evidence for a negative signal delivered through the mannose receptor. *J. Immunol.* 166:7477–7485.
22. Joiner, K.A., S.A. Fuhrman, H.M. Miettinen, L.H. Kasper, and I. Mellman. 1990. *Toxoplasma gondii*: fusion competence of parasitophorous vacuoles in Fc receptor-transfected fibroblasts. *Science.* 249: 641–646.
23. Blander, J.M., and R. Medzhitov. 2004. Regulation of phagosome

maturation by signals from toll-like receptors. *Science*. 304:1014–1018.
24. Mordue, D.G., and L.D. Sibley. 1997. Intracellular fate of vacuoles containing *Toxoplasma gondii* is determined at the time of formation and depends on the mechanism of entry. *J. Immunol.* 159:4452–4459.
25. Bouvier, G., A.-M. Benoliel, C. Foa, and P. Bongrand. 1994. Relationship between phagosome acidification, phagosome- lysosome fusion, and mechanism of particle ingestion. *J. Leukoc. Biol.* 55:729–734.
26. Zimmerli, S., M. Majeed, M. Gustavsson, O. Stendahl, D.A. Sanan, and J.D. Ernst. 1996. Phagosome-lysosome fusion is a calcium-independent event in macrophages. *J. Cell Biol.* 132:49–61.
27. Kang, B.K., and L.S. Schlesinger. 1998. Characterization of mannose receptor-dependent phagocytosis mediated by *Mycobacterium tuberculosis* lipoarabinomannan. *Infect. Immun.* 66:2769–2777.
28. Speert, D.P., and S.C. Silverstein. 1985. Phagocytosis of unopsonized zymosan by human monocyte-derived macrophages: Maturation and inhibition by mannan. *J. Leukoc. Biol.* 38:655–658.
29. Chatterjee, D., K. Lowell, B. Rivoire, M.R. McNeil, and P.J. Brennan. 1992. Lipoarabinomannan of *Mycobacterium tuberculosis*. Capping with mannosyl residues in some strains. *J. Biol. Chem.* 267:6234–6239.
30. Kaur, D., T.L. Lowary, V.D. Vissa, D.C. Crick, and P.J. Brennan. 2002. Characterization of the epitope of anti-lipoarabinomannan antibodies as the terminal hexaarabinofuranosyl motif of mycobacterial arabinans. *Microbiology*. 148:3049–3057.
31. Ezekowitz, R.A., K. Sastry, P. Bailly, and A. Warner. 1990. Molecular characterization of the human macrophage mannose receptor: demonstration of multiple carbohydrate recognition-like domains and phagocytosis of yeasts in Cos-1 cells. *J. Exp. Med.* 172:1785–1794.
32. Downey, G.P., R.J. Botelho, J.R. Butler, Y. Moltyaner, P. Chien, A.D. Schreiber, and S. Grinstein. 1999. Phagosomal maturation, acidification, and inhibition of bacterial growth in nonphagocytic cells transfected with FcgammaRIIA receptors. *J. Biol. Chem.* 274:28436–28444.
33. Clemens, D.L., and M.A. Horwitz. 1995. Characterization of the *Mycobacterium tuberculosis* phagosome and evidence that phagosomal maturation is inhibited. *J. Exp. Med.* 181:257–270.
34. Vergne, I., J. Chua, H.H. Lee, M. Lucas, J. Belisle, and V. Deretic. 2005. Mechanism of phagolysosome biogenesis block by viable *Mycobacterium tuberculosis*. *Proc. Natl. Acad. Sci. USA*. 102:4033–4038.
35. Fiani, M.L., J. Beitz, D. Turvy, J.S. Blum, and P.D. Stahl. 1998. Regulation of mannose receptor synthesis and turnover in mouse J774 macrophages. *J. Leukoc. Biol.* 64:85–91.
36. Stahl, P.D., and R.A. Ezekowitz. 1998. The mannose receptor is a pattern recognition receptor involved in host defense. *Curr. Opin. Immunol.* 10:50–55.
37. Stahl, P., P.H. Schlesinger, E. Sigardson, J.S. Rodman, and Y.C. Lee. 1980. Receptor-mediated pinocytosis of mannose glycoconjugates by macrophages: characterization and evidence for receptor recycling. *Cell.* 19:207–215.
38. Stein, M., S. Keshav, N. Harris, and S. Gordon. 1992. Interleukin 4 potently enhances murine macrophage mannose receptor activity: a marker of alternative immunologic macrophage activation. *J. Exp. Med.* 176:287–292.
39. Montaner, L.J., R.P. Da Silva, J. Sun, S. Sutterwala, M. Hollinshead, D. Vaux, and S. Gordon. 1999. Type 1 and type 2 cytokine regulation of macrophage endocytosis: differential activation by IL-4/IL-13 as opposed to IFN-γ or IL-10. *J. Immunol.* 162:4606–4613.
40. DeFife, K.M., C.R. Jenney, A.K. McNally, E. Colton, and J.M. Anderson. 1997. Interleukin-13 induces human monocyte/macrophage fusion and macrophage mannose receptor expression. *J. Immunol.* 158:3385–3390.
41. Goerdt, S., and C.E. Orfanos. 1999. Other functions, other genes: alternative activation of antigen-presenting cells. *Immunity*. 10:137–142.
42. Tailleux, L., O. Schwartz, J.L. Herrmann, E. Pivert, M. Jackson, A. Amara, L. Legres, D. Dreher, L.P. Nicod, J.C. Gluckman, et al. 2003. DC-SIGN is the major *Mycobacterium tuberculosis* receptor on human dendritic cells. *J. Exp. Med.* 197:121–127.
43. Koppel, E.A., I.S. Ludwig, M.S. Hernandez, T.L. Lowary, R.R. Gadikota, A.B. Tuzikov, C.M. Vandenbroucke-Grauls, Y. van Kooyk, B.J. Appelmelk, and T.B. Geijtenbeek. 2004. Identification of the mycobacterial carbohydrate structure that binds the C-type lectins DC-SIGN, L-SIGN and SIGNR1. *Immunobiology*. 209:117–127.
44. Figdor, C.G., Y. van Kooyk, and G.J. Adema. 2002. C-type lectin receptors on dendritic cells and Langerhans cells. *Nat. Rev. Immunol.* 2:77–84.
45. Kruskal, B.A., K. Sastry, A.B. Warner, C.E. Mathieu, and R.A.B. Ezekowitz. 1992. Phagocytic chimeric receptors require both transmembrane and cytoplasmic domains from the mannose receptor. *J. Exp. Med.* 176:1673–1680.
46. Schweizer, A., P.D. Stahl, and J. Rohrer. 2000. A di-aromatic motif in the cytosolic tail of the mannose receptor mediates endosomal sorting. *J. Biol. Chem.* 275:29694–29700.
47. Puig-Kroger, A., D. Serrano-Gomez, E. Caparros, A. Dominguez-Soto, M. Relloso, M. Colmenares, L. Martinez-Munoz, N. Longo, N. Sanchez-Sanchez, M. Rincon, et al. 2004. Regulated expression of the pathogen receptor dendritic cell-specific intercellular adhesion molecule 3 (ICAM-3)-grabbing nonintegrin in THP-1 human leukemic cells, monocytes, and macrophages. *J. Biol. Chem.* 279:25680–25688.
48. Bernardo, J., A.M. Billingslea, R.L. Blumenthal, K.F. Seetoo, E.R. Simons, and M.J. Fenton. 1998. Differential responses of human mononuclear phagocytes to mycobacterial lipoarabinomannans: role of CD14 and the mannose receptor. *Infect. Immun.* 66:28–35.
49. Malik, Z.A., C.R. Thompson, S. Hashimi, B. Porter, S.S. Iyer, and D.J. Kusner. 2003. Cutting edge: *Mycobacterium tuberculosis* blocks $Ca^{(2+)}$ signaling and phagosome maturation in human macrophages via specific inhibition of sphingosine kinase. *J. Immunol.* 170:2811–2815.
50. Malik, Z.A., G.M. Denning, and D.J. Kusner. 2000. Inhibition of $Ca^{(2+)}$ signaling by *Mycobacterium tuberculosis* is associated with reduced phagosome-lysosome fusion and increased survival within human macrophages. *J. Exp. Med.* 191:287–302.
51. Schlesinger, L.S., T.M. Kaufman, S. Iyer, S.R. Hull, and L.K. Marciando. 1996. Differences in mannose receptor-mediated uptake of lipoarabinomannan from virulent and attenuated strains of *Mycobacterium tuberculosis* by human macrophages. *J. Immunol.* 157:4568–4575.
52. Rastogi, N., V. Labrousse, and J. Paulo Carvalho de Sousa. 1992. Mycobacterial growth and ultrastructure in mouse L-929 fibroblasts and bone marrow-derived macrophages: evidence that infected fibroblasts secrete mediators capable of modulating bacterial growth in macrophages. *Curr. Microbiol.* 25:203–213.
53. Chatterjee, D., and K.-H. Khoo. 1998. Mycobacterial lipoarabinomannan: an extraordinary lipoheteroglycan with profound physiological effects. *Glycobiology*. 8:113–120.
54. Ilangumaran, S., S. Arni, M. Poincelet, J.-M. Theler, P.J. Brennan, N. Din, and D.C. Hoessli. 1995. Integration of mycobacterial lipoarabinomannans into glycosylphosphatidylinositol-rich domains of lymphomonocytic cell plasma membranes. *J. Immunol.* 155:1334–1342.
55. Siddiqui, M.R., S. Meisner, K. Tosh, K. Balakrishnan, S. Ghei, S.E. Fisher, M. Golding, N.P.S. Narayan, T. Sitaraman, U. Sengupta, et al. 2001. A major susceptibility locus for leprosy in India maps to chromosome 10p13. *Nat. Genet.* 27:439–441.
56. Eichbaum, Q., P. Clerc, G. Bruns, F. McKeon, and R.A.B. Ezekowitz. 1994. Assignment of the human macrophage mannose receptor gene (MRC1) to 10p13 by *in situ* hybridization and PCR-based somatic cell hybrid mapping. *Genomics*. 22:656–658.
57. Torrelles, J.B., K.-H. Khoo, P.A. Sieling, R.L. Modlin, N. Zhang, A.M. Marques, A. Treumann, C.D. Rithner, P.J. Brennan, and D. Chatterjee. 2004. Truncated structural variants of lipoarabinomannan in *Mycobacterium leprae* and an ethambutol-resistant strain of *Mycobacterium tuberculosis*. *J. Biol. Chem.* 279:41227–41239.
58. Lemassu, A., and M. Daffé. 1994. Structural features of the exocellular polysaccharides of *Mycobacterium tuberculosis*. *Biochem. J.* 297:351–357.
59. Kielian, M.C., and Z.A. Cohn. 1980. Phagosome-lysosome fusion. Characterization of intracellular membrane fusion in mouse macrophages. *J. Cell Biol.* 85:754–777.
60. Taylor, M.E., J.T. Conary, M.R. Lennartz, P.D. Stahl, and K. DrickAm. 1990. Primary structure of the mannose receptor contains multiple motifs resembling carbohydrate-recognition domains. *J. Biol. Chem.* 265:12156–12162.